Electronic Supplementary Material (ESI) for Sustainable Energy & Fuels.
This journal is © The Royal Society of Chemistry 2019

Supplementary information for

Cobalt-based ferrites as efficient redox materials for thermochemical two-step CO_2-splitting: enhanced performance due to cation diffusion

Jincheng Huang,[a, b, c] Yu Fu,[a] Shuqing Li,[a] Wenbo Kong,[a] Jun Zhang*[a] and Yuhan Sun*[a, d]

[a] CAS Key Laboratory of Low-Carbon Conversion Science and Engineering, Shanghai Advanced Research Institute, Chinese Academy of Science, Shanghai 201203, PR China

[b] Key Laboratory of Optoelectronic Devices and Systems of Ministry of Education and Guangdong Province, Shenzhen University, Shenzhen 518060, PR China

[c] University of Chinese Academy of Sciences, Beijing 100049, PR China

[d] School of Physical Science and Technology, ShanghaiTech University, Shanghai 201203, PR China

Table S1 The distribution of Co and Fe ion at different sites

sample	Fraction (%)					
	Co2p			Fe2p		
	octahedral site	tetrahedral site	ratio (R)	octahedral site	tetrahedral site	ratio (R)
as-synthesized $CoFe_2O_4/CoO$	62.95	37.05	1.70	61.13	38.87	1.57
spent $CoFe_2O_4/CoO$	57.04	42.96	1.33	42.10	57.90	0.73
as-synthesized $CoFe_2O_4/ZrO_2$	57.17	42.83	1.34	63.50	36.50	1.74
spent $CoFe_2O_4/ZrO_2$	72.43	27.57	2.63	62.56	37.44	1.67
as-synthesized $CoFe_2O_4/Al_2O_3$	40.69	59.31	0.69	61.76	38.24	1.61
spent $CoFe_2O_4/Al_2O_3$	56.61	43.39	1.30	61.26	38.74	1.58

R: the ratios of ions at octahedral to tetrahedral sites

Table S2 Mössbauer parameters of the $CoFe_2O_4$-based material

sample	Hf (kOe)	IS (mm/s)	QS (mm/s)	Γ/2 (mm/s)	Area (%)
as-synthesized $CoFe_2O_4$/CoO	490.20	0.47	-0.01	0.34	48.2
	469.46	0.42	0.00	0.19	23.5
	434.28	0.52	-0.05	0.45	28.3
spent $CoFe_2O_4$/CoO	507.50	0.51	0.03	0.33	37.1
	487.94	0.42	0.00	0.21	50.0
	457.60	0.70	-0.24	0.54	12.9
as-synthesized $CoFe_2O_4/Al_2O_3$	515.21	0.38	0.19	0.21	38.8
	469.80	0.29	0.02	0.31	38.1
	425.04	0.32	0.00	0.47	23.1
spent $CoFe_2O_4/Al_2O_3$	491.94	0.52	0.00	0.27	29.4
	471.79	0.42	-0.01	0.20	37.0
	445.79	0.51	0.00	0.34	33.6

H_f: magnetic hyperfine field, IS: isomer shift, QS: quadruple split, Γ/2: half width at half maximum

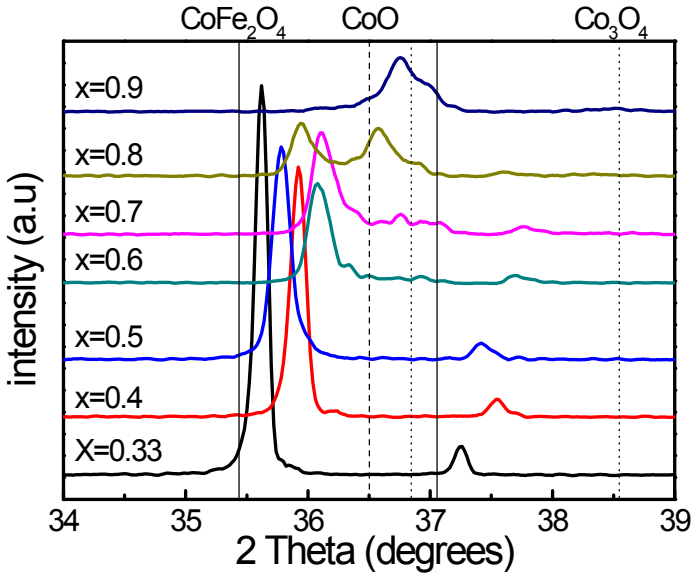

Figure S1. XRD traces of as-synthesized Co-based ferrites.

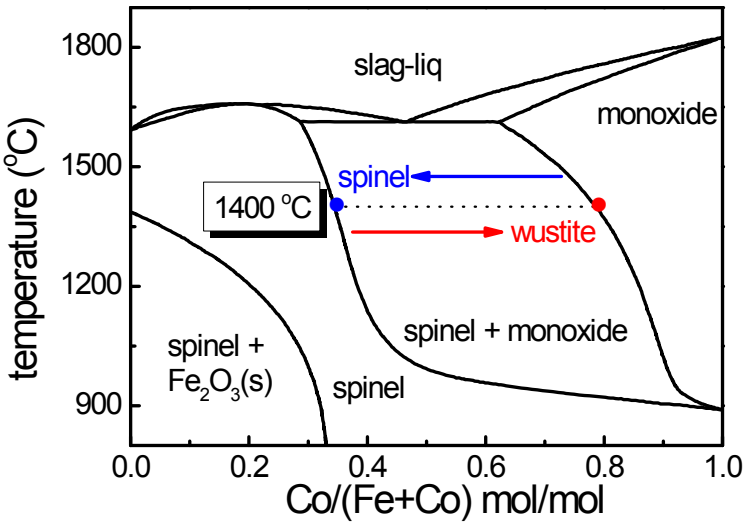

Figure S2. Phase diagram corresponding to compositions *vs* temperature of Co-Fe-O system ($P(O_2)$ = 0.21 atm). The phase diagram shows the evolution of the phase change when temperature and composition changes. In addition, the phase diagram indicates that the fraction of wüstite phase increases as the increasing of Co content.

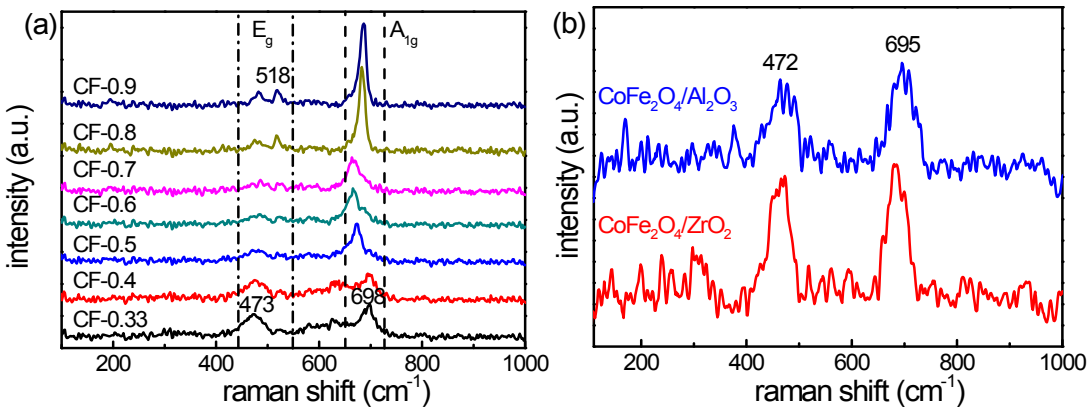

Figure S3. Raman spectra of the as-synthesized (a) CF-x and (b) $CoFe_2O_4$-based materials.

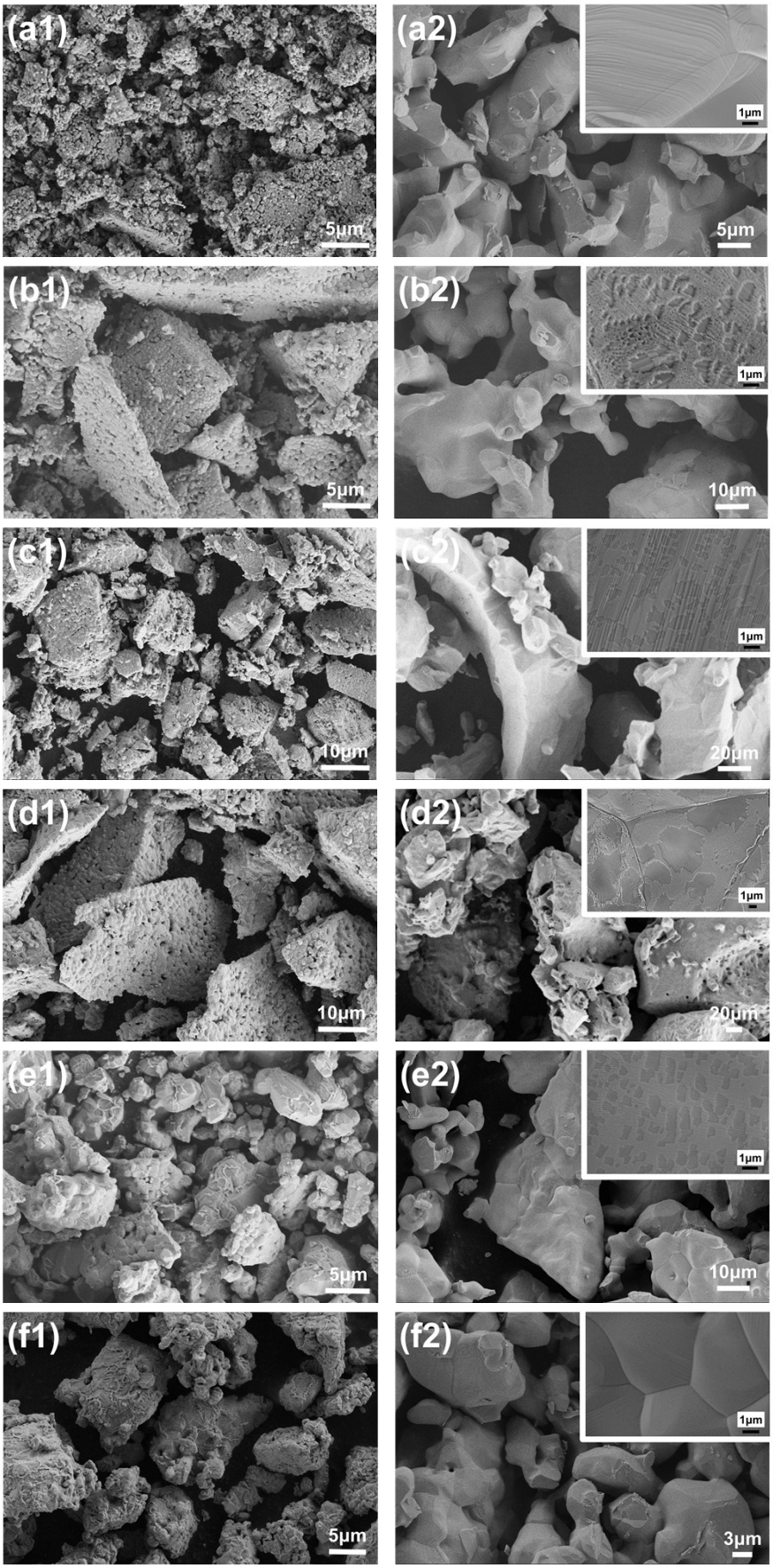

Figure S4. SEM images of Co-based ferrites: (a) CF-0.33, (b) CF-0.4, (c) CF-0.6, (d) CF-0.7, (e) CF-0.8, (f) CF-0.9. 1 and 2 represent the as-synthesized and spent sample, respectively.

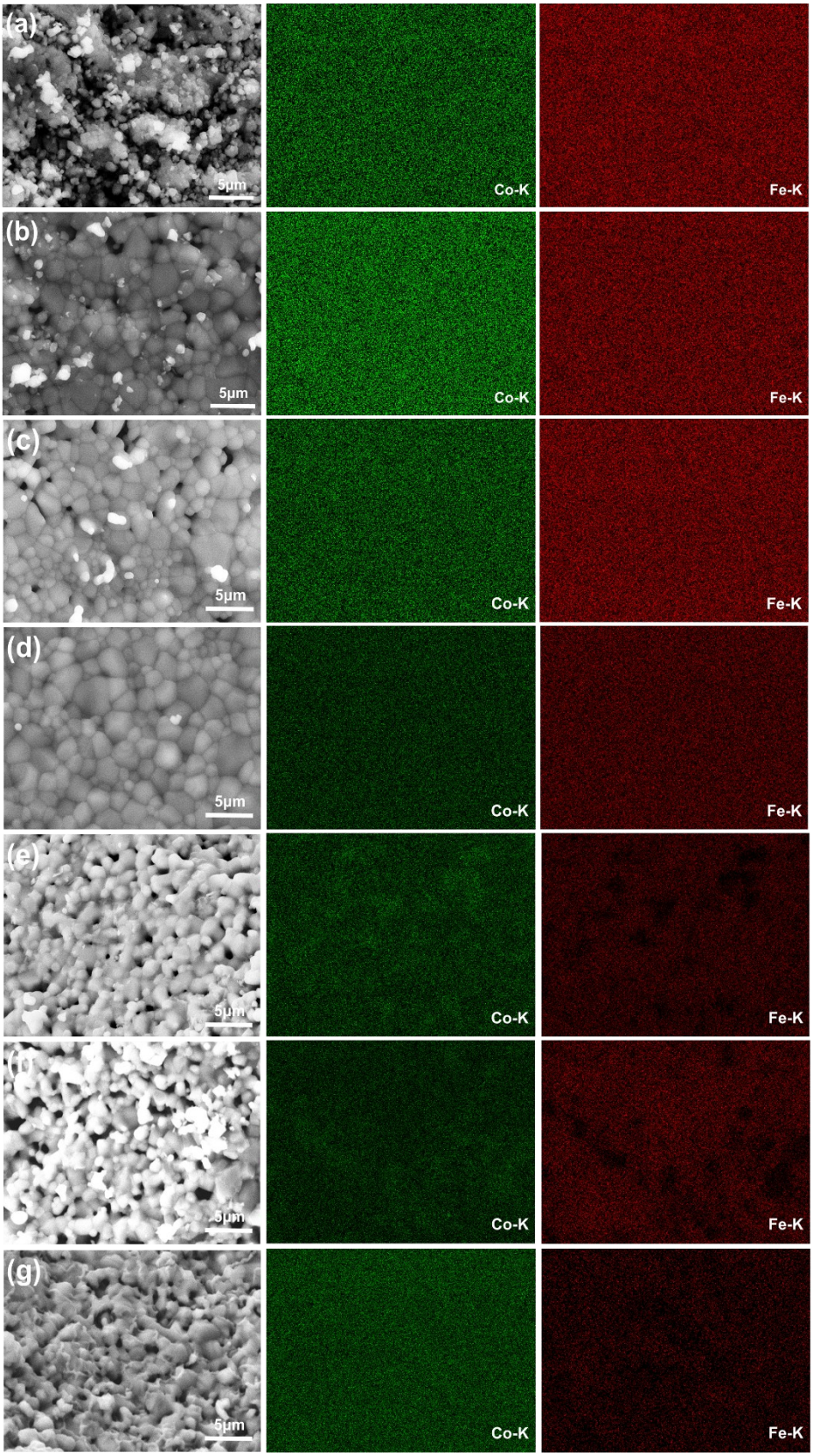

-Figure S5. The SEM images and corresponding energy disperse spectrum (zone-scan) images of as-synthesized Co-based ferrites, (a) x = 0.33, (b) x = 0.4, (c) x =0.5, (d) x = 0.6, (e) x = 0.7, (f) x = 0.8, (g) x = 0.9.

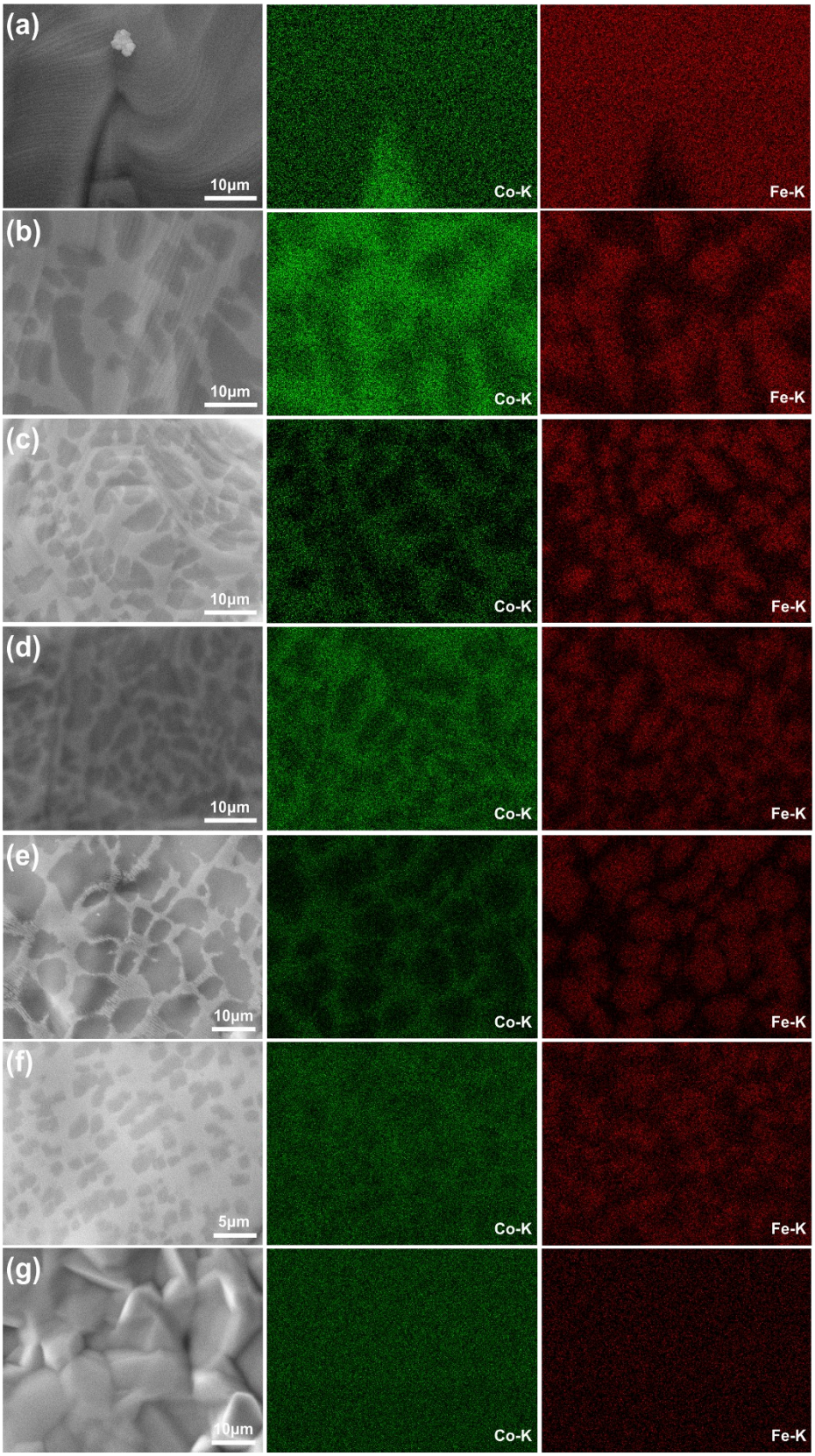

Figure S6. The SEM images and corresponding energy disperse spectrum (zone-scan) images of spent Co-based ferrites, (a) x = 0.33, (b) x = 0.4, (c) x =0.5, (d) x = 0.6, (e) x = 0.7, (f) x = 0.8, (g) x = 0.9.

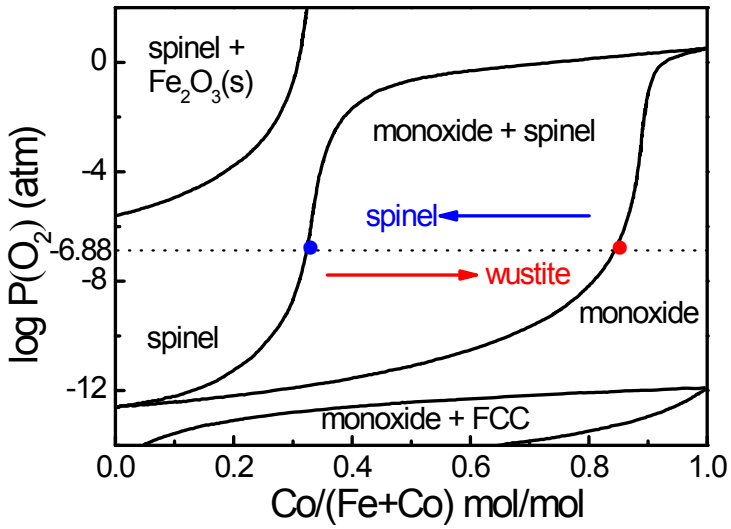

Figure S7. Phase diagram corresponding to compositions *vs* oxygen chemical potential of Co-Fe-O system (temperature =1000 ^{o}C). In the actual thermal reduction step of the redox reaction, the oxygen partial pressure is about 1.33 ×10^{-7} atm, corresponding to a log P(O_2) value of -6.88. And under this oxygen chemical potential, the fraction of wüstite phase increases as the increasing of Co content.

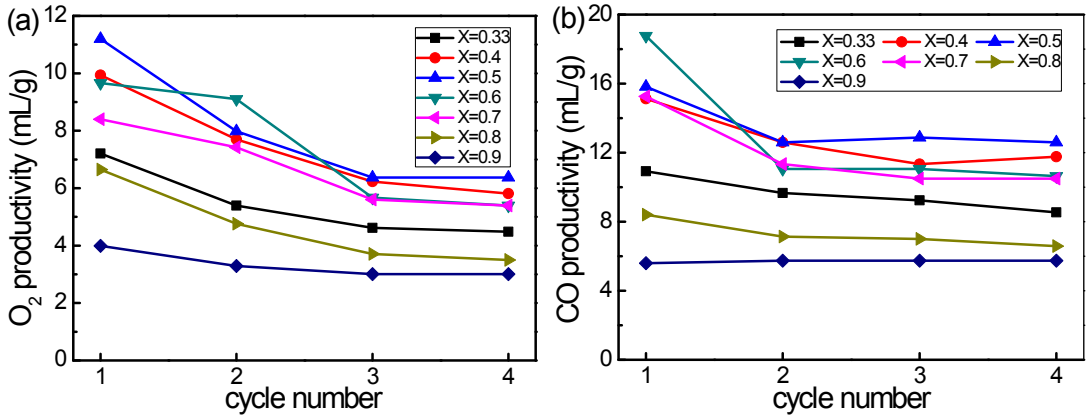

Figure S8. Thermal reduction and CO_2 splitting activity of Co-based ferrites: (a) O_2 productivity, (b) CO productivity. The data were derived from the mass variation of the TGA curves.

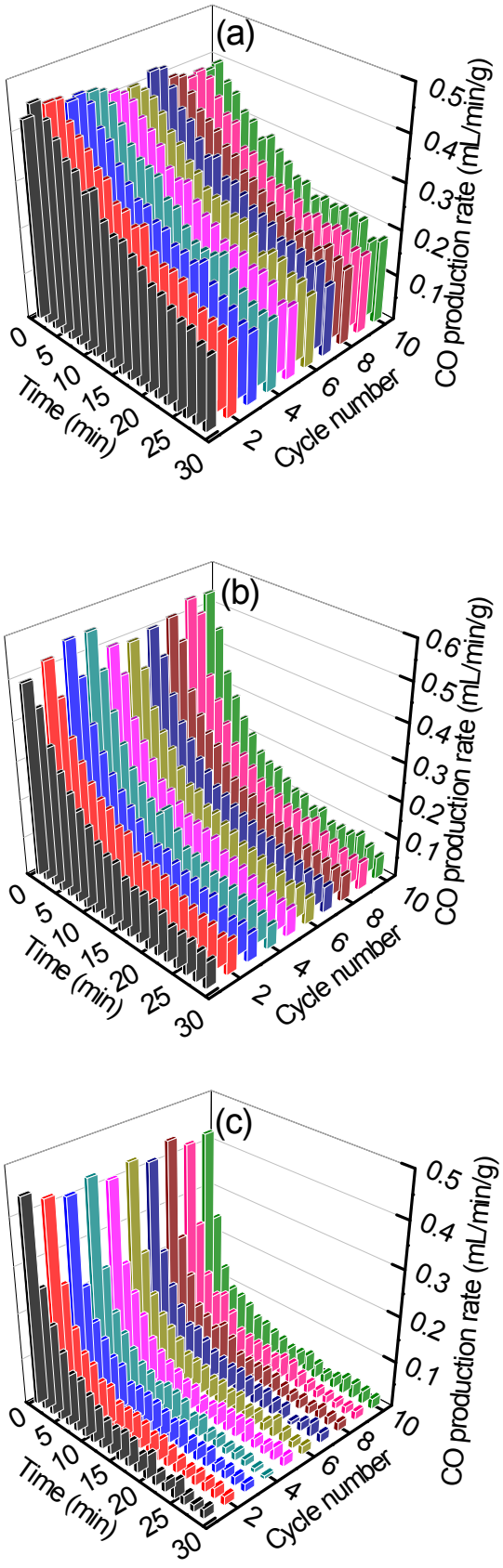

Figure S9. The CO production rate as a function of time over ten cycles: (a) $CoFe_2O_4/CoO$, (b) $CoFe_2O_4/ZrO_2$, (c) $CoFe_2O_4/Al_2O_3$

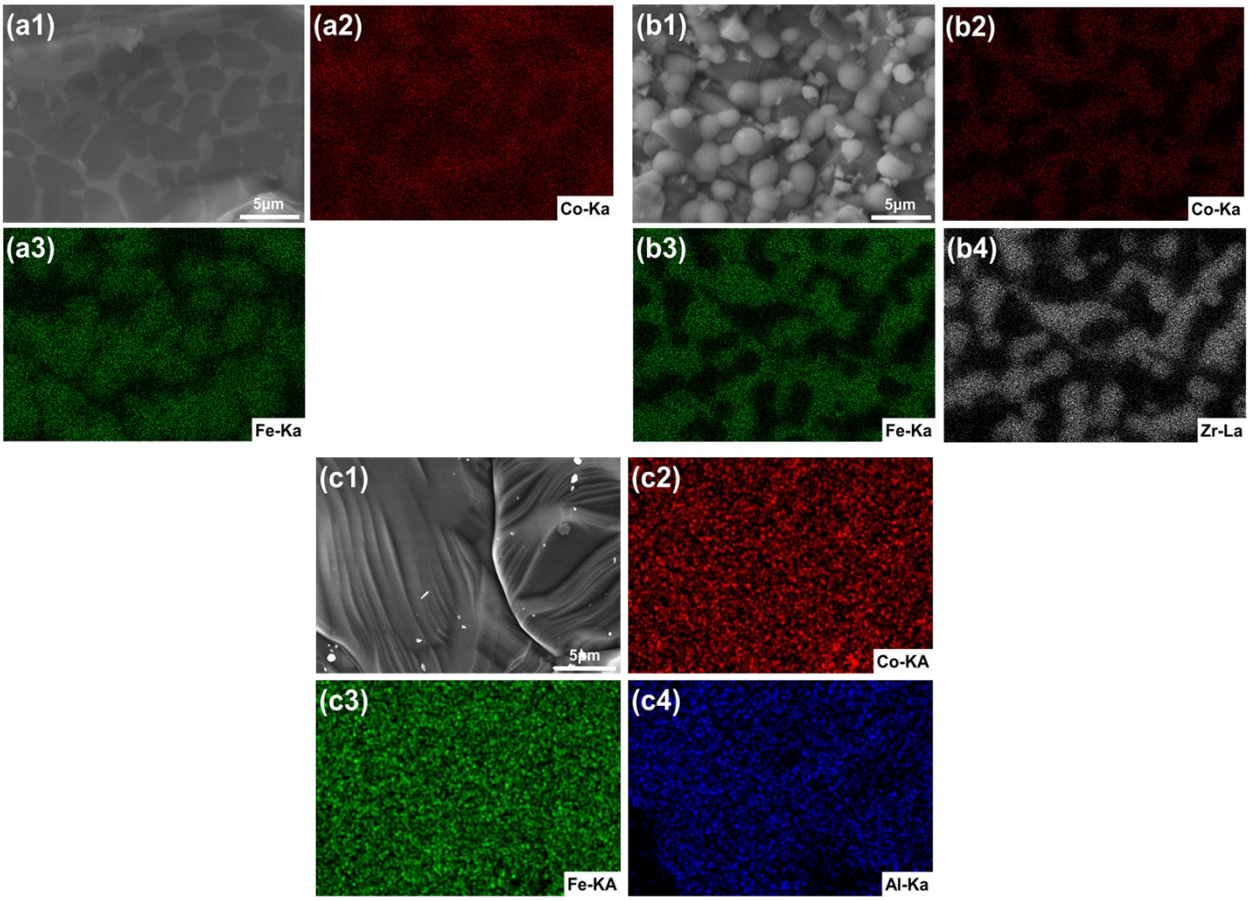

Figure S10. The zone-scan of EDS analysis of the spent $CoFe_2O_4$-based material: (a) $CoFe_2O_4$/CoO, (b) $CoFe_2O_4/ZrO_2$, (c) $CoFe_2O_4/Al_2O_3$.

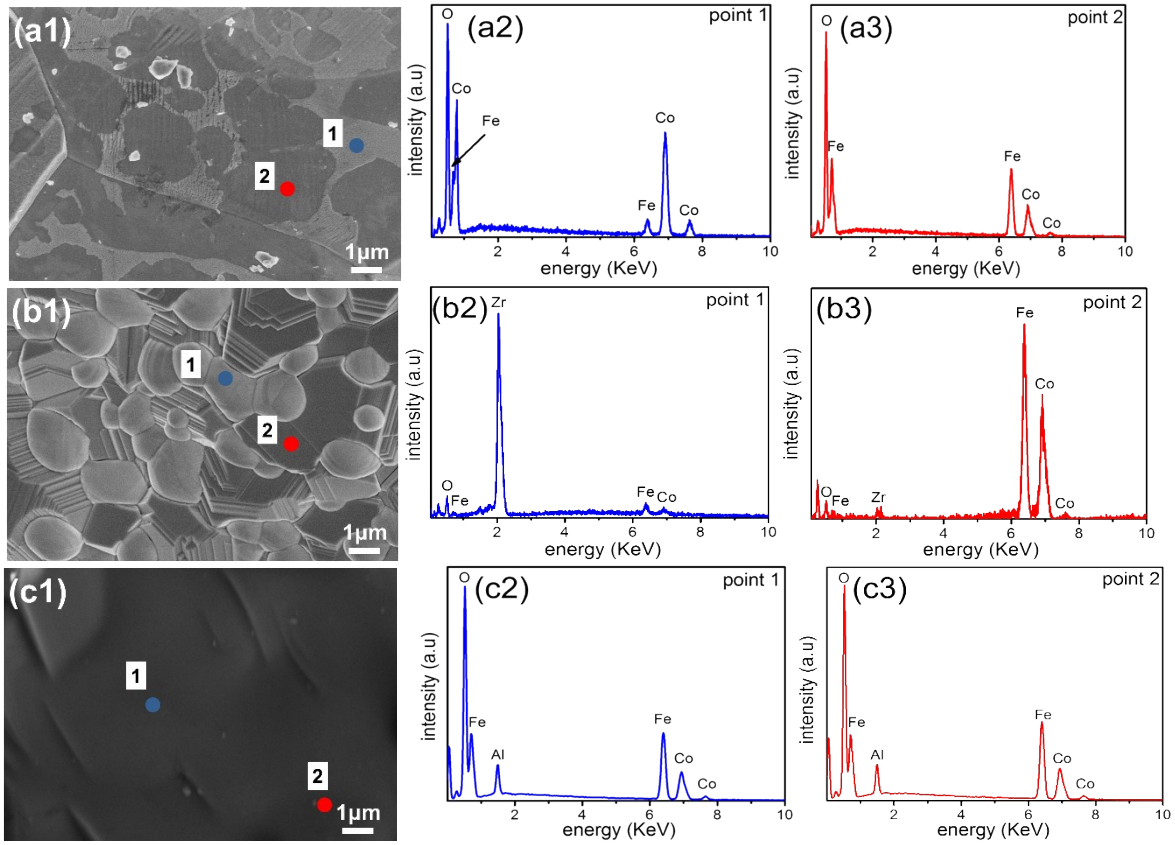

Figure S11. The dot-scan of EDS analysis of the spent $CoFe_2O_4$-based material: (a) $CoFe_2O_4$/CoO, (b) $CoFe_2O_4/ZrO_2$, (c) $CoFe_2O_4/Al_2O_3$.

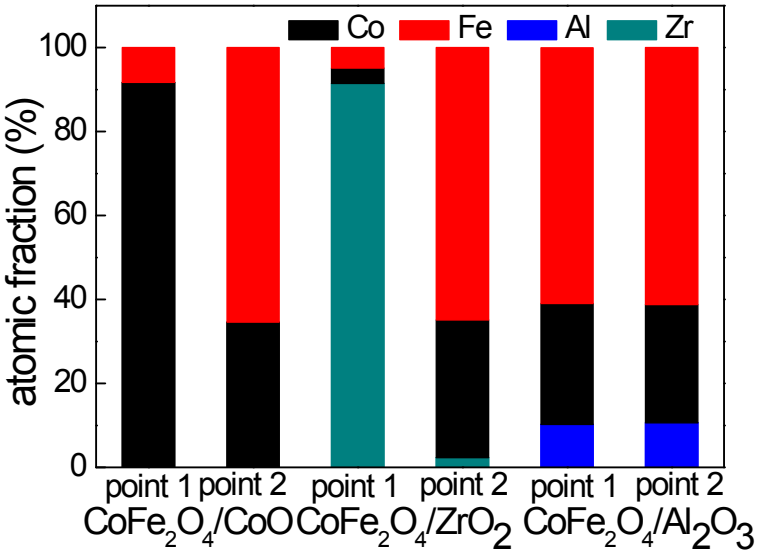

Figure S12. The atomic percentages of ions near the surface of $CoFe_2O_4$-based materials after 10 redox cycles, data were derived from the EDS analysis.